Eur. J. Pharmacol. **204**, 339 (1991).
7. J. Zhang and S. H. Snyder, *Proc. Natl. Acad. Sci. U.S.A.* **89**, 9382 (1992); A. Y. Kots *et al.*, *FEBS Lett.* **300**, 9 (1992); S. Dimmeler, F. Lottspeich, B. Brune, *J. Biol. Chem.* **267**, 16771 (1992); L. Molina y Vedia *et al.*, *ibid.*, p. 24929. McDonald and Moss demonstrated that NO-enhanced modification of GAPDH by [^{32}P]NAD is a covalent bond between NAD and a thiol residue in GAPDH [L. J. McDonald and J. Moss, *Proc. Natl. Acad. Sci. U.S.A.* **90**, 6238 (1993)].
8. J.-C. Drapier and J. B. Hibbs Jr., *J. Clin. Invest.* **78**, 790 (1986).
9. M. Lepoivre *et al.*, *J. Biol. Chem.* **265**, 14143 (1990); N. S. Kwon *et al.*, *J. Exp. Med.* **174**, 761 (1991).
10. D. A. Wink *et al.*, *Science* **254**, 1001 (1991).
11. T. Nguyen *et al.*, *Proc. Natl. Acad. Sci. U.S.A.* **89**, 3030 (1992).
12. G. de Murcia, J. Menissier-de Murcia, V. Schreiber, *Bioessays* **13**, 455 (1991); J. E. Cleaver and W. F. Morgan, *Mutat. Res.* **257**, 1 (1991).
13. J. C. Gaal *et al.*, *Trends Biol. Sci.* **12**, 129 (1987); N. A. Berger, *Radiat. Res.* **101**, 4 (1985).
14. Whole brains from 1-day-old rats were homogenized in 20% (w/v) buffer A [50 mM tris-HCl (pH 7.4), 1 mM EDTA, 1 mM dithiothreitol, 50 mM NaCl, 0.25 M sucrose, 0.2 mM phenylmethylsulfonyl fluoride, and the inhibitors chymostatin, leupeptin, pepstatin, and trypsin (1 μg/ml of each)]. The homogenate was centrifuged at 1000*g* for 15 min. The pellet was washed with buffer A and centrifuged again. The washed pellet, termed nuclear fraction, was resuspended in buffer A. PARS activity was assayed according to Schranfstatter *et al.* [*J. Clin. Invest.* **77**, 1312 (1986)]. Each 50-μl assay mixture contained 10 μg of the nuclear protein fraction and [*adenylate*-^{32}P]NAD (0.1 mM, 10 Ci/mmol), in the presence or absence of 4-amino-1,8-naphthalimide (20 μM), 1,5-dihydroxyisoquinoline (20 μM), benzamide (100 μM), SNP (1 mM), SIN-1 (1 mM), DNA (0.1 pg, pTrcA, InVitrogen), and DNA that had been treated with NO gas, SNP, or SIN-1. Incubation of DNA with NO gas was according to (*11*). DNA treated with SNP and SIN-1 doubled PARS activity, but neither compound had an effect on PARS by itself. When [^{14}C]NADs were used in place of [^{32}P]NAD in PARS assays, radioactive polymers were only formed from [*adenine*-^{14}C]NAD, not from [*carbonyl*-^{14}C]NAD.
15. To test whether NO interacts directly with benzamide, we incubated benzamide (1 mM) with SNP (1 mM) for 30 min, 1 hour, and 5 days at 25°C and analyzed it by high-pressure liquid chromatography (HPLC) on a C_{18} column. Benzamide treated with SNP was 100% recovered at the same elution time point with the same ultraviolet spectrum as that of untreated benzamide. When SNP-treated benzamide and benzamide were mixed and analyzed, only one peak was observed. Benzamide, at 0.03, 0.1, 0.3, and 1 mM, did not compete with cytochrome c for being reduced by superoxide generated from xanthine and xanthine oxidase.
16. The IC_{50} for benzamide in inhibiting PARS in vitro is 22 μM [M. Banasik, H. Komura, M. Shimoyama, K. Ueda, *J. Biol. Chem.* **267**, 1569 (1992)]. In intact cells, a higher value would be anticipated because benzamide would be competing with millimolar endogenous concentrations of NAD [R. McNerney *et al.*, *Biochim. Biophys. Acta* **1009**, 185 (1989)].
17. R. D. Randall and S. A. Thayer, *J. Neurosci.* **12**, 1882 (1992); D. W. Choi, *Neuron* **1**, 623 (1988); *J. Neurosci.* **10**, 2493 (1990).
18. Nitrite formation in a human kidney 293 cell line stably transfected with the cDNA for brain NOS was measured in response to A23187 (10 μM) as described [D. S. Bredt, C. D. Ferris, S. H. Snyder, *J. Biol. Chem.* **267**, 10976 (1992)]. A23187 (10 μM) elicited the formation of 17.1 ± 2.1 μM nitrite in 2 hours. Benzamide (100 μM) did not prevent the formation of nitrite (15.9 ± 3.8 μM nitrite), and 100 μM nitroarginine diminished nitrite formation to 3.9 ± 1.6 μM nitrite (mean ± SEM, n = 3).
19. See, for example, O. H. Lowry *et al.*, *J. Biol. Chem.* **239**, 18 (1964); D. Uematsu *et al.*, *Brain Res.* **482**, 129 (1989); K. M. Raley and P. Lipton, *Neurosci. Lett.* **110**, 118 (1990).
20. B. Meldrum and J. Garthwaite, *Trends Pharmacol. Sci.* **11**, 379 (1990).
21. B. Kallman *et al.*, *Life Sci.* **51**, 671 (1992).
22. Primary neuronal cultures from cortex were prepared from fetal Sprague-Dawley rats, gestation day 13 to 14. Mature neurons (more than 21 days in culture) were used in all experiments. We determined neurotoxicity by exposing the neurons to the various test solutions as described (*4*). NMDA, SNP, or SNAP were applied to the cells for 5 min, then the cells were washed and replaced with minimum essential medium and 21 mM glucose overnight in the incubator. After 20 to 24 hours of exposure to test solutions, the neurons were exposed to 0.4% Trypan blue in control salt solution to stain the residue of nonviable cells and to assess toxicity. Viable and nonviable cells were counted. At least two separate experiments using four separate wells were done for each data point shown. Significant overall values were obtained with a one-way, between-groups analysis of variance. Specific comparisons on all possible pair combinations were made with the Student's t test for independent means.
23. We thank S. Pou (Department of Pharmacology and Toxicology, University of Maryland School of Pharmacy) for NO, R. Henning (Leiter Der Pharma-Forschung, Cassella A.G., Frankfurt, Germany) for providing SIN-1, H. Zhou for providing purified pTrcA, and N. Bruce for manuscript preparation. Supported by USPHS grants DA-00266, contract DA-271-90-7408, Research Scientist Award DA-00074 (S.H.S.), a grant from Asahi Chemical Company, and a grant of the W. M. Keck Foundation. T.M.D. was supported by USPHS Clinical Investigator Development Award NS-01578 and a grant from the American Academy of Neurology. V.L.D. was supported by an Intramural Research Training Award from NIH.

5 August 1993; accepted 13 December 1993

Adenosine Inhibition of Mesopontine Cholinergic Neurons: Implications for EEG Arousal

Donald G. Rainnie, Heinz C. R. Grunze, Robert W. McCarley, Robert W. Greene*

Increased discharge activity of mesopontine cholinergic neurons participates in the production of electroencephalographic (EEG) arousal; such arousal diminishes as a function of the duration of prior wakefulness or of brain hyperthermia. Whole-cell and extracellular recordings in a brainstem slice show that mesopontine cholinergic neurons are under the tonic inhibitory control of endogenous adenosine, a neuromodulator released during brain metabolism. This inhibitory tone is mediated postsynaptically by an inwardly rectifying potassium conductance and by an inhibition of the hyperpolarization-activated current. These data provide a coupling mechanism linking neuronal control of EEG arousal with the effects of prior wakefulness, brain hyperthermia, and the use of the adenosine receptor blockers caffeine and theophylline.

Factors as diverse as prior wakefulness, brain hyperthermia, and adenosine blockers [such as caffeine and theophylline (*1*)] control the degree of arousal, usually measured as EEG activation (EEG arousal). Both the propensity to sleep and the intensity of delta waves upon falling asleep are proportional to the duration of prior wakefulness (*2*, *3*). Behavioral experiments have shown that a rise in brain temperature induces somnolence and a high level of EEG delta activity during sleep (*4*). The stimulating effects of coffee (caffeine) and tea (theophylline) are a nearly universal subjective experience, one whose EEG arousal effects have been documented (*5*). However, the neural mediator or mediators of the effects of these diverse events on EEG arousal are unknown.

Considerable evidence suggests that mesopontine cholinergic neurons play a key role in EEG arousal (*6*, *7*). The cholinergic neurons of this region form a continuum, extending from the laterodorsal tegmental nucleus (LDT) laterally to the pedunculopontine tegmental nucleus (PPT); they project heavily to the forebrain and thalamus in rat, cat, and monkey (*8*). In vivo extracellular data indicate that a majority of these cholinergic neurons selectively discharge during states of EEG arousal (*7*). Furthermore, both in vivo and in vitro data indicate that the cholinergic neurons promote EEG arousal by a cholinergic depolarization of thalamic neurons that, when hyperpolarized, oscillate in the delta EEG frequency range in concert with their cortical neuronal targets (*6*).

It seemed likely, therefore, that modulation of mesopontine cholinergic activity might be a key neural mediator of behavioral state. Adenosine (AD) was of particular interest as a modulator of these neurons because (i) the production and release of AD into the extracellular media is linked to neuronal metabolic activity (*9*); (ii) neural metabolism is much greater during wakefulness than in delta sleep and is also increased by hyperthermia (*10*); and (iii) caffeine and

Department of Psychiatry, Harvard University and Brockton Veterans Administration Medical Center, Brockton, MA 02401.

*To whom correspondence should be addressed.

theophylline are powerful blockers of electrophysiologically relevant AD receptors (*11*). We report that endogenous AD exerted a strong inhibitory tone on identified cholinergic LDT-PPT neurons in an in vitro brainstem slice preparation.

Previous data on specific antagonism of AD receptor sites had suggested the presence of a tonic influence of endogenous AD in several regions of the central nervous system (*12*). Consequently, we first examined the effects of both AD antagonists and exogenous AD on network excitability as measured by extracellularly recorded firing rates in the LDT-PPT and the diagonal band of Broca (DBB) in vitro (*13*). The DBB is part of the cholinergic basal forebrain complex that innervates the cortex (*8*). In response to superfusion of the specific AD antagonist 8-cyclopentyl-1,3-dimethylxanthine (CPT) (*14*), the average baseline firing rate of 2.14 ± 3.75 Hz was significantly increased to 4.31 ± 5.71 Hz ($P \leq 0.005$; $n = 19$) in the LDT-PPT. The increase persisted for the duration of drug application and returned to baseline levels after washout (Fig. 1A). Exogenous application of AD caused a significant ($P \leq 0.025$) decrease in firing frequency in this and all neurons tested (baseline firing rate, 3.7 ± 5.9 Hz; with AD, 1.8 ± 3.5 Hz; $n = 9$). Similar results were obtained in the DBB [baseline firing rate, 2.9 ± 3.2 Hz; with CPT (10 μM), 5.3 ± 3.6 Hz; $P \leq 0.005$; $n = 12$]. Furthermore, in all LDT-PPT and DBB neurons tested, the addition of 8-*p*-sulphotheophylline (8-*p*-ST) (50 μM), a lipophobic AD antagonist (*15*), caused a significant increase in firing rate ($P \leq 0.005$, $n' = 9$ in LDT-PPT; $P \leq 0.025$, $n = 6$ in DBB) similar to that evoked by CPT (Fig. 1, B and C).

We used whole-cell patch recordings of LDT neurons (*13*) to examine the postsynaptic mechanisms contributing to this increase in excitability. In voltage clamp, CPT evoked a small inward, voltage-dependent current (Fig. 1D). Both the voltage sensitivity and the kinetics of this response were characteristic of a hyperpolarization-activated current, I_h (*16*). The latter was apparent as a slowly activating inward relaxation evoked by transient hyperpolarizing step commands (500 ms, −50 mV) from a holding potential (V_h) of −60 mV. Exposure to CPT (10 μM) enhanced this inward relaxation (Fig. 1D, inset). All neurons of the LDT expressed I_h; however, the extent of expression varied from neuron to neuron. These data suggested that CPT removed a tonic endogenous AD inhibition of I_h and that I_h might be further inhibited by exposure to exogenous AD, as reported in thalamic neurons (*17*).

Indeed, exogenous AD (20 μM) reduced I_h in all LDT neurons examined (Fig. 2A; $n = 9$) (*13*). In voltage clamp, transient (500-ms) hyperpolarizing step commands of increasing amplitude (−10 to −50 mV) resulted in the activation of an inward relaxation dependent on time and voltage (Fig. 2A, upper trace). In the presence of AD, the inward relaxation was reduced (*18*) (Fig. 2A, lower trace). There also was an increase in the magnitude of a low-threshold inward Ca^{2+} current, I_t, in association with the block of the slow I_h tail current seen upon termination of the hyperpolarizing step command (*19*). The amplitude of the I_h inward relaxation was calculated by the subtraction of $I_{instantaneous}$ from $I_{steady\ state}$ and was plotted as a function of membrane potential to provide an estimate of the magnitude of I_h (Fig. 2B). The reduction of I_h by AD was most obvious at hyperpolarized membrane potentials. To reduce possible contamination by the AD-activated inward rectifier, we examined the effects of AD application (20 μM) in the presence of barium (500 μM, $n = 3$). The inwardly rectifying current induced by AD was blocked; however, there was no effect on I_h (*16*). In the presence of barium, AD evoked a small outward current with a *V-I*

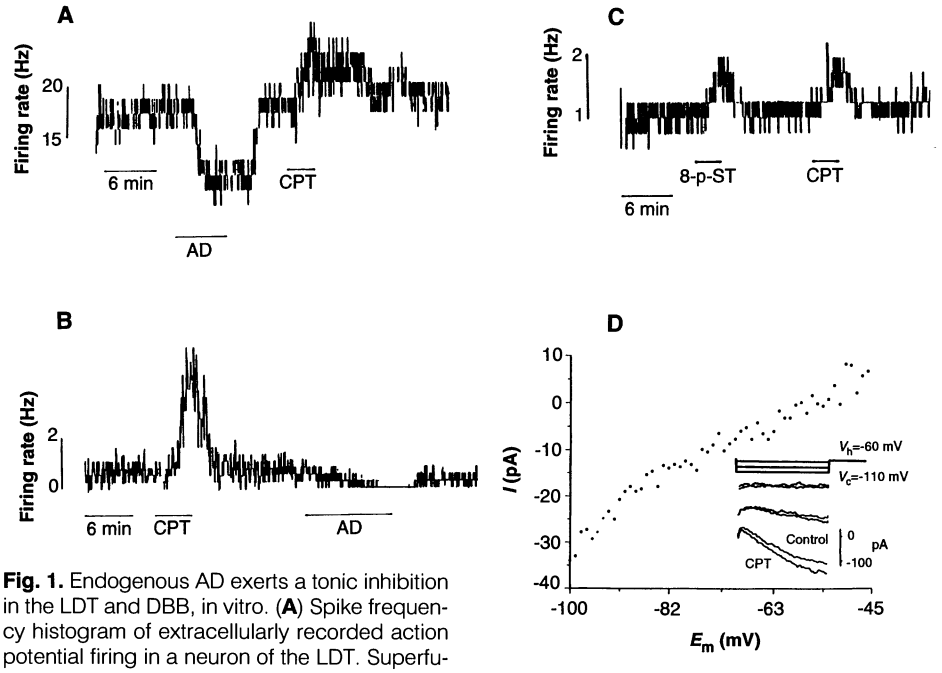

Fig. 1. Endogenous AD exerts a tonic inhibition in the LDT and DBB, in vitro. (**A**) Spike frequency histogram of extracellularly recorded action potential firing in a neuron of the LDT. Superfusion with AD (100 μM) causes a marked reduction of firing frequency and CPT (10 μM) causes a prolonged increase in firing frequency. (**B**) In the DBB, application of CPT (10 μM) similarly increases firing rates, and subsequent exogenous AD decreased firing rates. (**C**) Application of 8-*p*-ST (50 μM) mimics the effect of CPT in an LDT neuron. (**D**) Whole-cell voltage-clamp recording of the response of a histochemically identified LDT cholinergic neuron to CPT application. E_m, membrane potential. Digital subtraction of steady-state voltage-current relations obtained before and during CPT (10 μM) reveals a CPT-induced current with voltage and kinetic characteristics of I_h. (**Inset**) Enhanced inward relaxation during CPT application. The relatively hyperpolarized reversal potential for I_h may reflect a small additional presynaptic input evoked by CPT.

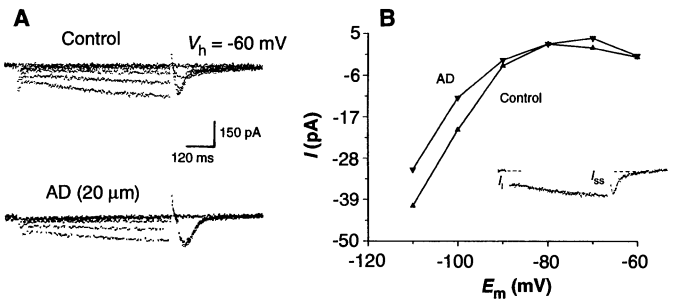

Fig. 2. Exogenous AD application reduces an inwardly relaxing I_h current in LDT neurons. (**A**) Current traces of an LDT neuron before and during AD application. Voltage step commands (−10 to −50 mV; 500 ms) from a holding potential of −60 mV reveal a slow inwardly relaxing current of increasing amplitude (upper traces). The presence of AD (20 μM) reduces the expression of the inward relaxation (lower traces). (**B**) A plot of the voltage-current relation determined for the inward relaxation before and during AD application. (**Inset**) The inward relaxation current (I_{relax}) was calculated by subtraction of the instantaneous current (I_i) from the steady-state current (I_{ss}) for each of the current traces in (A).

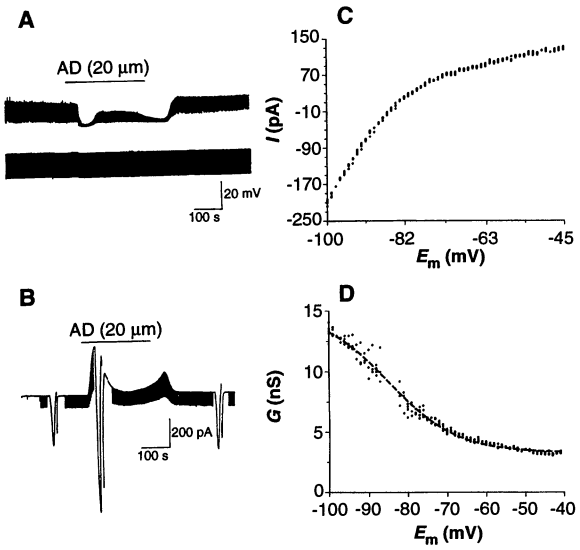

Fig. 3. Exogenous AD application evokes a membrane hyperpolarization mediated by activation of an inwardly rectifying K^+ conductance in neurons of the LDT. (**A**) In a whole-cell current-clamp recording, AD evokes a membrane hyperpolarization and an associated decrease in membrane input resistance. (**B**) Current trace from another neuron voltage clamped at V_h = −60 mV. Application of AD evokes an outward current and an associated increase in membrane conductance. Downward deflections in (A) and (B) reflect the voltage and current response to 100-pA, 20-mV hyperpolarizing step commands 200 ms in duration that were used to determine the resistance and conductance. (**C**) A plot of AD current as a function of membrane potential reveals AD activation of an inwardly rectifying K^+ conductance. AD current was calculated by digital subtraction of the current evoked by "ramping" the neuron from −100 to −40 mV [see (B)] in control from that obtained during AD application. (**D**) AD chord conductance G as a function of membrane potential is well fit by a Boltzmann equation (dashed line) with a half-activation potential $V_{1/2}$ of −85 mV and a slope factor of k = 9 [same neuron as in (C)].

relation (over the range −100 to −40 mV) consistent with an antagonism of I_h.

Bath application of AD (5 to 100 μM) produced an additional inhibitory response of greater magnitude than the reduction of I_h in 52 of 72 neurons tested. Responses were characterized by a predominant hyperpolarization associated with a decrease in membrane input resistance (*20*) (Fig. 3A). Similar effects were observed in voltage-clamp mode at a holding potential V_h = −60 mV (Fig. 3B).

We obtained *V-I* ramps (from −100 to −40 mV at a rate of 1 mV/s) before and during the AD response to determine the voltage sensitivity of the AD-induced conductance changes (Fig. 3B). The AD-induced current was calculated by digital subtraction of the control *V-I* ramp from the *V-I* ramp in the presence of AD (Fig. 3C). In every responsive neuron examined, the AD current showed marked inward rectification, with the current being greater at more hyperpolarized potentials and with an average (±SD) reversal potential of −82 ± 4 mV (n = 10). The plot of adenosine chord conductance $[I_{AD}/(E_m - E_{reversal})]$ as a function of membrane potential (Fig. 3D, dots) was well fit by the Boltzmann equation (Fig. 3D, dashed line) with a half-activation potential $V_{1/2}$ = −85 mV and steepness factor of k = 9.

The responses to AD persisted in Ringer solution containing low concentrations of calcium (0.2 mM) and high concentrations of magnesium (10 mM), blocking synaptic transmission (n = 4). They were blocked by bath application of CPT (500 nm to 10 μM; n = 12). In addition, application of the specific A_1 receptor agonist, N^6-cyclohexyladenosine (CHA) (50 nM; n = 4) (*21*) evoked a long-lasting monophasic hyperpolarization mediated by activation of an inwardly rectifying K^+ conductance with properties similar to those of the conductance evoked by AD.

Dual labeling experiments showed that 60% of intracellularly labeled AD-responsive LDT neurons stained positively for reduced nicotinamide adenine dinucleotide phosphate (NADPH)–diaphorase and were thus cholinergic (*22*). The 28% of LDT neurons that did not respond to AD did respond to other neurotransmitters such as acetylcholine (10 μM) with a characteristic monophasic hyperpolarization (*23, 24*).

Together, these findings support the presence of a significant inhibitory tone mediated by AD on the cholinergic neurons of the mesopontine tegmentum (LDT-PPT) and in the DBB. This inhibition in the LDT-PPT is mediated, at least in part, by an inhibition of I_h and by activation of an inwardly rectifying potassium conductance (*25*). These effects may act in concert to reduce the excitability of the neurons as well as increase their tendency to burst. The inhibition of I_h would remove the I_h-mediated shunt of the burst current, I_t (Fig. 2) (*19*), and facilitate the removal of inactivation of I_t (*26*), as would the AD activation of the inwardly rectifying K^+ conductance.

Because brainstem and basal forebrain cholinergic neurons are likely to have an integral role in thalamocortical arousal (*6*), factors affecting extracellular AD levels may be predicted to affect the behavioral state of arousal. Manipulations of central nervous system tissue that either increase metabolic demand or decrease metabolic substrate availability result in increased AD production and extracellular AD levels (*9*). During wakefulness, when cholinergic neuronal activity is high (*7*), increased metabolic activity (*9, 10*) may cause an increase in both intracellular and extracellular AD. Accumulation of intracellular AD may further increase extracellular AD by altering the transmembrane AD gradient to reduce facilitated transport of AD into the cell (*27*).

Consequently, extracellular AD builds up and increasingly inhibits those cholinergic neurons important for arousal. Similar functionally localized AD effects may occur in other regions of the central nervous system, and indeed, diurnal variations of AD levels in the frontal cortex have been reported (*28*). However, this local inhibition of cholinergic neurons would be especially powerful in alteration of behavioral state because of their widespread and strategic efferent targets in the thalamic and cortical systems important for the control of EEG arousal (*5*). This adenosinergic sleep factor would thus decrease EEG activity, increase drowsiness, and promote EEG delta-wave activity during subsequent sleep.

We further suggest that extracellular AD levels decrease during the reduced metabolic activity of sleep, especially delta-wave sleep, a time when cholinergic neurons are relatively quiescent (*7*); this postulate is congruent with the observed declining exponential time course of delta-wave activity over a night's sleep (*29*). Supporting this line of reasoning is the strong evidence that increasing cerebral metabolic rate by hyperthermia increases sleepiness and delta activity. There is suggestive evidence that even sustained mental activity may have the same result (*3*), although measurement of extracellular AD in vivo in correlation with behavioral state remains to be done. In demonstrating the powerful inhibitory tone of AD on neurons important in control of EEG arousal, these data put forward cellular pharmacologic evidence for the long-sought coupling mechanism that links neuronal control of EEG arousal to the effects of prior wakefulness.

REFERENCES AND NOTES

1. The behavioral effects of caffeine and theophylline seem to derive from their activity as adenosine antagonists [inhibition constant K_i < 60 μM for the A_1 and A_2 receptors; A. Sattin and T. W. Rall, *Mol. Pharmacol.* **6**, 13 (1970); F. Pons, F. Bruns, J. W. Daly, *J. Neurochem.* **34**,,1319 (1980); S. H. Snyder, *Annu. Rev. Neurosci.* **8**, 103 (1985)] rather than their activity as either phosphodiesterase inhibitors [constant for 50% inhibition IC_{50} > 350 μM; O. H. Choi, M. T. Shamin, W. L. Padgett, J. W. Daly, *Life Sci.* **43**, 387 (1988)] or mediators of intracellular calcium release [median effective

concentration EC_{50} = 6 mM; P. S. McPherson *et al.*, *Neuron* **7**, 17 (1991); K. Kuba, *J. Physiol.* **298**, 547 (1980); I. R. Neering and R. N. McBurney, *Nature* **309**, 158 (1984); D. D. Freil and R. W. Tsien, *J. Physiol.* **450**, 217 (1992)].
2. A. A. Borbély, *Hum. Neurobiol.* **1**, 195 (1982); I. Feinberg *et al.*, *Electroencephalogr. Clin. Neurophysiol.* **61**, 134 (1985).
3. J. Horne, *Experientia* **48**, 941 (1992).
4. D. McGinty and R. Szymusiak, *Trends Neurosci.* **13**, 480 (1990).
5. G. Yanik, S. Glaum, M. Radulovacki, *Brain Res.* **403**, 177 (1987); R. B. Virus *et al.*, *Neuropsychopharmacology* **3**, 243 (1990).
6. M. Steriade, D. A. McCormick, T. J. Sejnowski, *Science* **262**, 679 (1993).
7. M. Steriade, S. Datta, D. Paré, G. Oakson, R. Curró Dossi, *J. Neurosci.* **10**, 2541 (1990); M. Steriade, D. Paré, S. Datta, G. Oakson, R. Curró Dossi, *ibid.*, p. 2560.
8. M. Steriade, D. Paré, A. Parent, Y. Smith, *Neuroscience* **25**, 47 (1988); K. Semba and H. C. Fibiger, *Prog. Brain Res.* **79**, 37 (1989).
9. I. Pull and H. McIlwain, *Biochem. J.* **130**, 975 (1972); H. R. Winn, J. E. Welsh, R. Rubio, R. M. Berne, *Circ. Res.* **47**, 568 (1980); J. Schrader *et al.*, *Pflugers Arch.* **387**, 245 (1980); R. M. Berne *et al.*, in *Cerebral Hypoxia in the Pathogenesis of Migraine*, F. C. Rose and W. K. Amery, Eds. (Pitman, London, 1982), pp. 89–91; D. G. L. Van Wylen *et al.*, *J. Cereb. Blood Flow Metab.* **6**, 522 (1986); H. McIlwain and J. D. Poll, *J. Neurobiol.* **17**, 39 (1986).
10. In humans, a 44% reduction in the cerebral metabolic rate (CMR) of glucose during delta-wave sleep, compared with that during wakefulness, was determined by P. Maquet *et al.* [*Brain Res.* **571**, 149 (1992)], and a 25% reduction in the CMR of O_2 was determined by P. L. Madsen *et al.* [*J. Appl. Physiol.* **70**, 2597 (1991)]. Horne (*3*) has reviewed metabolism and hyperthermia.
11. T. V. Dunwiddie, B. J. Hoffer, B. B. Fredholm, *Naunyn Schmiedebergs Arch. Pharmacol.* **316**, 326 (1981); R. W. Greene, H. L. Haas, A. Hermann, *Br. J. Pharmacol.* **85**, 163 (1985).
12. For reviews, see T. V. Dunwiddie, *Int. Rev. Neurobiol.* **27**, 63 (1985); R. W. Greene and H. L. Haas, *Prog. Neurobiol.* **36**, 329 (1991).
13. Slices were obtained from anesthetized 14- to 21-day-old male and female Long-Evans rat pups and were prepared with standard procedures (*23*). Extracellular single units were recorded (electrode filled with modified Ringer solution had resistances from 12 to 15 megohms) with ac filtering, and spike rates were analyzed with a computer-generated window and spike-rate integration. Whole-cell recordings were obtained with the technique of M. G. Blanton, J. J. LoTurco, and A. R. Kriegstein [*J. Neurosci. Methods* **30**, 203 (1989)]. Briefly, borosilicate glass electrodes (resistance, 4 to 6 megohms) were filled with 100 mM potassium citrate, 20 mM KCl, 1 mM $CaCl_2$, 3 mM $MgCl_2$, 2 mM MgATP, 2 mM NaGTP, 3 mM EGTA, 40 mM Hepes, and biocytin (0.25%). Recordings were made with an Axoclamp 2A amplifier (Axon Instruments, Burlingame, CA) and Basic Fastlab software (Indec Systems, Sunnyvale, CA). Voltage-clamp records were obtained in discontinuous voltage-clamp mode at a switching frequency of 2.5 to 4.0 kHz. Head-stage output was continuously monitored to ensure adequate settling in each duty cycle. Neurons filled with 0.25% biocytin were visualized with standard procedures and processed for reduced nicotinamide adenine dinucleotide phosphate (NADPH)–diaphorase histochemistry (*30*). Data are expressed as mean ± SD, and significance was determined by Wilcoxon signed-rank test.
14. The CPT K_i = 10.9 nM at A_1 receptors, and at A_2 receptors, K_i = 1440 nM; R. F. Bruns, *J. Biochem. Pharmacol.* **30**, 325 (1981).
15. The 8-*p*-ST K_i = 2630 nM at A_1 receptors, and at A_2 receptors, K_i = 15,300 nM; R. F. Bruns, J. W. Daly, S. H. Snyder, *Proc. Nat. Acad. Sci. U.S.A.* **77**, 5547 (1980).
16. J. V. Halliwell and P. R. Adams, *Brain Res.* **250**, 71 (1983); M. L. Mayer and G. L. Westbrook, *J. Physiol.* **340**, 19 (1983). In LDT neurons, I_h was also blocked by extracellular application of cesium (2 mM; n = 3). In the presence of cesium, which itself increased firing rates (n = 4), the increase in firing rate evoked by CPT was reduced by 87 ± 23%.
17. H. C. Pape, *J. Physiol.* **447**, 729 (1992).
18. For examination of the effect of AD on I_h, neurons were required to show an appreciable inward relaxation ≥10 pA after a −40-mV step command from V_h = −60 mV.
19. Although a direct effect resulting from an increase in the low-threshold Ca^{2+} current cannot be excluded, the increase is consistent with a reduced shunt caused by a decreased I_h [(*30*); A. Kamondi *et al.*, *J. Neurophysiol.* **68**, 1359 (1992)].
20. The inhibitory response was usually (>90%) triphasic, consisting of a hyperpolarization followed by a depolarization (but not a complete return to E_m) and then a subsequent hyperpolarization that persisted until removal of the AD. In many neurons, after washout of AD, the membrane potential returned to a point more depolarized than E_m. The triphasic composition could result from (i) A_1 receptor activation and subsequent activation of a non-A_1 receptor, (ii) deamination and subsequent saturation of the AD deaminase, (iii) delayed activation and saturation of an uptake pump, or (iv) a combination of these effects.
21. The CHA IC_{50} = 1 to 2 nM at A_1 receptors, and at A_2 receptors, IC_{50} = 450 to 1000 nM; R. F. Bruns *et al.*, *Mol. Pharmacol.* **29**, 331 (1986).
22. S. R. Vincent *et al.*, *Neurosci. Lett.* **43**, 31 (1983).
23. J. Leubke *et al.*, *J. Neurophysiol.* **70**, 2128 (1993).
24. D. G. Rainnie, H. C. R. Grunze, R. W. McCarley, R. W. Greene, unpublished data.
25. The observation that endogenous AD blocks primarily I_h is consistent with the notion that this pathway is most sensitive to AD receptor activation and that the most efficacious AD effect is activation of the inward rectifier.
26. D. A. McCormick and H. Pape, *J. Physiol. London* **431**, 291 (1990).
27. J. G. Gu and J. D. Geiger, *J. Neurochem.* **58**, 1699 (1992); P. H. Wu and J. W. Phyllis, *Neurochem. Int.* **6**, 613 (1984); J. D. Geiger and J. I. Nagy, in *Adenosine and Adenosine Receptors*, M. Williams, Ed. (Humana Press, Clifton, NJ, 1990). Other mechanisms that would similarly influence extracellular AD levels include modulation of AD anabolic and catabolic enzyme activity and AD transport rate constants or activities.
28. V. Chagoya de Sánchez *et al.*, *Brain Res.* **612**, 115 (1993).
29. This metabolic-dependent AD buildup and decay is consistent with a phenomenologically accurate mathematical model of delta-sleep buildup and decay (*2*), including the very subtle point that delta-wave propensity increases during rapid eye movement sleep, when brain metabolic activity is similar to that during wakefulness.
30. J. I. Luebke *et al.*, *Proc. Natl. Acad. Sci. U.S.A.* **89**, 743 (1992).

9 September 1993; accepted 8 December 1993

Associative Odor Learning in *Drosophila* Abolished by Chemical Ablation of Mushroom Bodies

J. Steven de Belle* and Martin Heisenberg

The corpora pedunculata, or mushroom bodies (MBs), in the brain of *Drosophila melanogaster* adults consist of ~2500 parallel Kenyon cell fibers derived from four MB neuroblasts. Hydroxyurea fed to newly hatched larvae selectively deletes these cells, resulting in complete, precise MB ablation. Adult flies developing without MBs behave normally in most respects, but are unable to perform in a classical conditioning paradigm that tests associative learning of odor cues and electric shock. This deficit cannot be attributed to reductions in olfactory sensitivity, shock reactivity, or locomotor behavior. The results demonstrate that MBs mediate associative odor learning in flies.

Common cellular processes underlie both associative and nonassociative learning in both invertebrate and vertebrate species (*1*). Beyond the realm of single cells, specialized neuronal assemblies have been implicated in the learning and storage of sensory information. In mammals, the hippocampus is important for the initial formation of declarative memory (*2*). In insects, MBs are assumed to play a role in the processing and storage of chemosensory information (*3*, *4*).

The relative simplicity and unusual shape of the MB neuropil (*5*) suggests that it has a specialized function. The primary input to the MBs is the antennal-glomerular tract (AGT), which extends from the antennal lobe (AL) to the lateral horn (LH) of the lateral protocerebrum (LPR) and sends a network of fibers into the MB calyx (*5*, *6*). At least in some insect species, the calyx also receives fibers from visual and other sensory systems (*5*, *6*) and, therefore, likely processes multimodal information. MB outputs extend from the lobes to many areas in the brain including the LPR. Some fibers provide feedback connections between the calyx, peduncle, and lobes, whereas other fibers connect the MBs to each other across the sagittal midplane (*5*).

In honeybees, local cooling of the MBs interrupts olfactory memory (*7*). Depolarization of a ventral unpaired medial neuron (VUMmx1) innervating the calyces of bees can supplant the unconditioned stimulus

Theodor-Boveri-Institut für Biowissenschaften, Lehrstuhl für Genetik, Universität Würzburg, Am Hubland, D-97074 Wurzburg, Germany.

*To whom correspondence should be addressed after 1 March 1994: Max-Planck-Institut für Biologische Kybernetik, Spemannstrasse 38, D-72076 Tübingen, Germany.